Critical test of the diffraction model in amorphous and disordered metals

L. V. Meisel and P. J. Cote
Benet Weapons Laboratory, Watervliet Arsenal, Watervliet, New York 12189
(Received 27 December 1977)

The transport properties of amorphous metals below their Debye temperatures Θ are examined within the framework of the diffraction model. The electrical resistivity ρ is predicted to exhibit the following features: (i) All curves deviate from their $T = 0$°K values as $+T^2$; (ii) Negative temperature coefficients of resistivity (TCR) occur at $T \approx \Theta$ for $K \approx K_p$, where K_p is the position of the principal peak in the structure factor $a(K)$ and $K = 2k_F$. Positive TCR occur at all T for K outside the vicinity of K_p, i.e., to the left- and right-hand sides of K_p; (iii) Small maxima in ρ (of the order of tenths of a percent) are seen for $K \approx K_p$. The position of the maximum shifts to lower temperatures as $K \to K_p$. The largest maximum occurs for the nearly flat curve; (iv) The amplitude of the variations of ρ, and the size of the maxima are sensitive to Θ and the sharpness of the main peak in $a(K)$; (v) For fixed Θ, the positions of the maxima in ρ generally approach Θ as the main peak in $a(K)$ becomes smaller; (vi) The curves which display only positive TCR are generally S shaped; (vii) The electron-to-atom ratio for negative TCR is estimated to range from $1.3\mathfrak{z}$ to $3\mathfrak{z}$. The predictions are compared with experimental findings in a variety of amorphous alloys. The agreement is excellent. The question of breakdown of the diffraction model is discussed; some of the apparent paradoxes seen in high-resistivity metals are resolved through a redefinition of saturation. The implications of these results for disordered and liquid metals are also discussed.

I. INTRODUCTION

Cote[1] and Guntherodt *et al.*[2] first suggested that the Evans, Greenwood, and Lloyd[3] formulation of Ziman liquid-metal theory,[4] which we shall refer to as *the diffraction model*, could be applied to amorphous metals. It was subsequently shown[5] that the magnitude, temperature dependence, and composition dependence of the resistivity and thermopower of amorphous NiP and related alloys at and above their Debye temperatures is correctly given by the diffraction model. The generally observed low-temperature T^2 dependence of resistivity and the $\pm T$ dependence at high temperatures in amorphous and disordered crystalline metals was also found to be a natural consequence of this model.[6,7] Furthermore, experimental evidence[8] confirmed that the temperature dependence of the x-ray static structure factor[7] (above the Debye temperature) is consistent with the measured temperature coefficients of resistivity (TCR) in NiP.[5]

Nevertheless, alternative theories, which are compatible with many of these general features of electrical transport, are often invoked.[9] In this paper we show that the diffraction model gives the *detailed* behavior of the electrical resistivity of glassy metals below the Debye temperature. The alternative theories do not explain these details.

II. THEORY

The resistivity of pure liquid metals is given by Evans, Greenwood, and Lloyd[3] as

$$\rho = \frac{12\pi\Omega_0}{e^2 h V_F^2} \int_0^1 d\left(\frac{K}{2k_F}\right)\left(\frac{K}{2k_F}\right)^3 S^\rho(K)\,|t(K)|^2 , \tag{1}$$

where Ω_0 is the atomic volume, V_F is the Fermi velocity, k_F is the Fermi wave vector, $\vec{K}$ is the scattering vector, h is Planck's constant divided by 2π, e is the electron charge, and the static structure factor for resistivity $S^\rho(K)$ is defined in terms of the Van Hove[10] dynamical structure factor $S(K,\omega)$ as

$$S^\rho(K) = \int_{-\infty}^{\infty} S(K,\omega)\, x n(x)\, d\omega , \tag{2}$$

where $x = h\omega/k_B T$ and $n(x) = (e^x - 1)^{-1}$. k_B is Boltzmann's constant and T is the absolute temperature. The t matrix is given by

$$t(K) = -\frac{2\pi h^3}{m(2mE_F)^{1/2}\Omega_0} \sum_l (2l+1)\sin\eta_l(E_F) \times e^{i\eta_l(E_F)} P_l(\cos\theta) , \tag{3}$$

where the phase shift $\eta_l(E_F)$ for angular-momentum quantum number l is evaluated at the Fermi energy E_F and m is the electron mass.

Meisel and Cote have shown[7] that in an amorphous Debye solid the resistivity structure factor can be expanded as

$$S^\rho(K) = S_0^\rho(K) + S_1^\rho(K) + S_2^\rho(K) + \cdots , \tag{4}$$

where $S_n^\rho(k)$ is an n-phonon term. The elastic term is

$$S_0^\rho(K) = a(K)\, e^{-2W(K)} , \tag{5}$$

where $e^{-2W(K)}$ is the Debye-Waller factor and

$$a(K)=\frac{1}{N}\sum_{m,n}\exp[i\vec{K}\cdot(\vec{m}-\vec{n})], \tag{6}$$

with $\vec{m},\vec{n}$ the averaged ionic positions. The one-phonon term is

$$S_1^\rho(K)=\alpha(K)\left(\frac{\Theta}{T}\right)\int_0^1\left(\frac{q}{q_D}\right)^2 d\left(\frac{q}{q_D}\right)n(x)[n(x)+1]\times\int\frac{d\Omega}{4\pi}\,a(|\vec{K}+\vec{q}|), \tag{7}$$

where $\alpha(K)\equiv 3(hK)^2e^{-2W(K)}/Mk_B\Theta$ with M the average ionic mass and q_D is the Debye wave number. For $T<\Theta$, $S_0^\rho+S_1^\rho$ gives an excellent approximation to S^ρ; however, for $T\gtrsim\Theta$ the multiphonon terms become significant; thus, the approximation to the multiphonon series given by Hernandez-Calderone *et al.*[11] is incorporated here. The static structure factor for resistivity becomes

$$S^\rho(K)=S_0^\rho(K)+S_1^\rho(K)+\{1-[1+2W(K)]e^{-2W(K)}\}, \tag{8}$$

where S_0^ρ and S_1^ρ are given by Eqs. (5) and (7), respectively, and the bracketed expression is the correction term of Hernandez-Calderone *et al.*[11]

For alloy systems the product $S^\rho(K)|t(K)|^2$ in Eq. (1) is replaced by a sum of concentration-dependent terms involving single-site t matrices of the individual constituents and partial-structure factors.[12] Equations (5), (7), and (8) are then interpreted as pertaining to partial structure factors $S_{ij}^\rho(K)$ in the generalized form of Eq. (1). Within the diffraction model, variations of resistivity with temperature at constant volume will be given by the changes in the resistivity structure factors with temperature; the t matrices play the role of weighting functions in the integral of Eq. (1) and are essentially temperature independent. In glassy metals, which generally contain transition metals, the dominant contribution to the resistivity comes from the backscattering region $K\approx 2k_F$ so that to a good approximation

$$\rho\propto S_{\mathrm{TM}}^\rho(2k_F), \tag{9}$$

where $S_{\mathrm{TM}}^\rho(2k_F)$ is the transition-metal partial-structure factor evaluated at $2k_F$. Equations (5) and (7)–(9) form the basis for our analysis of transport in amorphous metals.

Percus-Yevick hard-sphere structure factors,[13] which closely approximate the main peak for glassy metals and are convenient analytic functions, are used to define $a(K)$ in Eqs. (5)–(7). This is an excellent approximation. For example, Percus-Yevick hard-sphere structure factors approximate the main peak in amorphous NiP alloys[8] within a few percent.

We shall also consider the temperature-dependent averaged structure factors

$$A^X(K)\equiv\int_0^{q_D}dq\,q[n(x)+\tfrac{1}{2}]\times\int\frac{d\Omega}{4\pi}\,a(|\bar{K}+\bar{q}|)\times\left\{\int_0^{q_D}dq\,q[n(x)+1]\right\}^{-1}, \tag{10}$$

and

$$A^\rho(K)\equiv\int_0^{q_D}dq\,q^2n(x)+1]\times\int\frac{d\Omega}{4\pi}\,a(|\bar{K}+\bar{q}|)\times\left(\int_0^{q_D}dq\,q^2n(x)[n(x)+1]\right)^{-1}, \tag{11}$$

introduced in a previous publication[6]; these are useful in making comparisons with other structural models and in gaining insight into the temperature dependences of the static-structure factors. In terms of averaged structure factors the one-phonon resistivity structure factor becomes

$$S_1^\rho(K)=\alpha(K)\,(T/\Theta)^2A^\rho(K)\,I_2(\Theta/T), \tag{12}$$

where

$$I_2\left(\frac{\Theta}{T}\right)\equiv\int_0^{\Theta/T}dx\,x^2n(x)[n(x)+1]=\left(\frac{\Theta}{T}\right)^3\int_0^1 d\left(\frac{q}{q_D}\right)\left(\frac{q}{q_D}\right)^2n(x)[n(x)+1]. \tag{13}$$

Including first-order thermal-diffuse scattering, the static-structure factor for x-ray scattering becomes

$$S^X(K)=a(K)\,e^{-2W(K)}+A^X(K)(1-e^{-2W(K)}). \tag{14}$$

It was shown[7] that in the low-T limit, $A^\rho(K)\to a(K)$ with deviations going as $(T/\Theta)^2$ and for $T\gtrsim\Theta$, $A^\rho(K)\approx A^X(K)$.

III. NUMERICAL RESULTS

(a) Static structure factor for resistivity[7,14]: Computed $S^\rho(T)/S^\rho(\Theta)$ for a variety of K values is displayed in Figs. 1–3. (N.B. the static structure factors are functions of T *and* K. The K variable is suppressed in the sequel.)

The parameters selected for the curves in Fig. 1 are representative of amorphous NiP, which is the basis of many ternary metallic glasses. Those of Fig. 2 are representative of CuZr.[9] Figure 3 gives results for a packing fraction which yields a relatively smooth structure factor

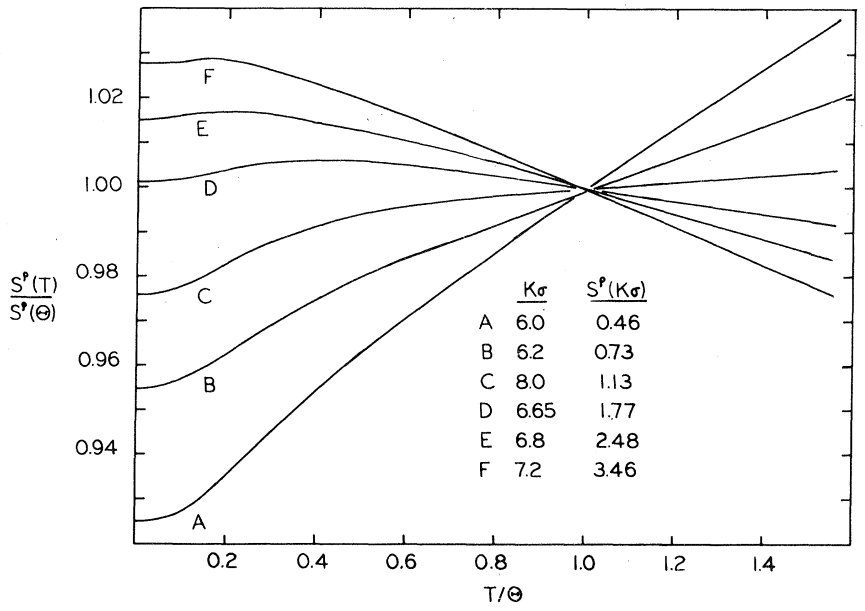

FIG. 1. Computed $S^\rho(T)/S^\rho(\Theta)$ for a variety of $K\sigma$ values, where $\eta = 0.525$, and $\Theta = 340$K. (The packing fraction η and the hard sphere diameter σ define the Percus-Yevick structure factor and K is the scattering vector, e.g., in amorphous NiP, $\sigma_{Ni} \approx 2.5$ Å.)

and is intended to simulate short-range-order peaks in disordered crystalline alloys.[15] These curves may be directly related to electrical resistivity via Eq. (9). [Replace $S^\rho(T)/S^\rho(\Theta)$ by $\rho(T)/\rho(\Theta)$ and identify the parameter K with $2k_F$.]

The curves exhibit the following characteristic features: (i) all curves deviate from their $T = 0$ values as $+T^2$; (ii) negative slopes occur at $T \approx \Theta$ for $K \approx K_p$, where K_p is the position of the principal peak in $a(K)$. Positive slopes occur at all T for K outside the vicinity of K_p, i.e., to the left and right of K_p; (iii) small maxima (of the order of tenths of a percent) are seen for $K \approx K_p$. The position of the maximum shifts to lower temperatures as $K \to K_p$. The largest maximum occurs for the nearly flat curve; (iv) the amplitude of the variations of $S^\rho(T)$, and the size of the maxima are sensitive to Θ and the sharpness of the main peak in $a(K)$; (v) for fixed Θ, the positions of the maxima in $S^\rho(T)$ generally approach Θ as the main peak in $a(K)$ becomes smaller; and (vi) the curves which display only positive slopes are generally S shaped.

(b) Average structure factor: Figure 4 shows the averaged structure factors $A^\rho(K)$ and $A^X(K)$ for a variety of temperatures. The parameters are representative of NiP. The zero temperature limit for $A^\rho(K)$ is $a(K)$ as expected[7]; however, the previously suggested[7] $A^\rho(K) \approx 1$ for

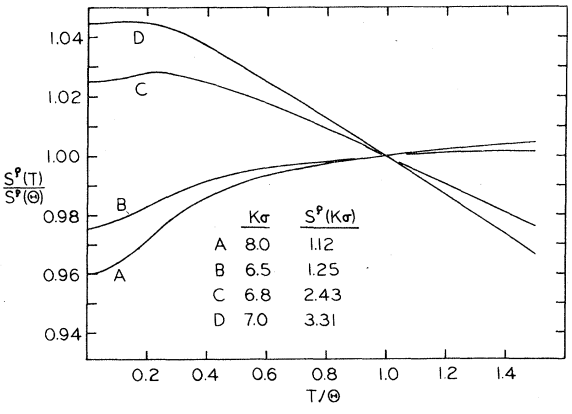

FIG. 2. Computed $S^\rho(T)/S^\rho(\Theta)$ for $\eta = 0.525$ and $\Theta = 200$ K.

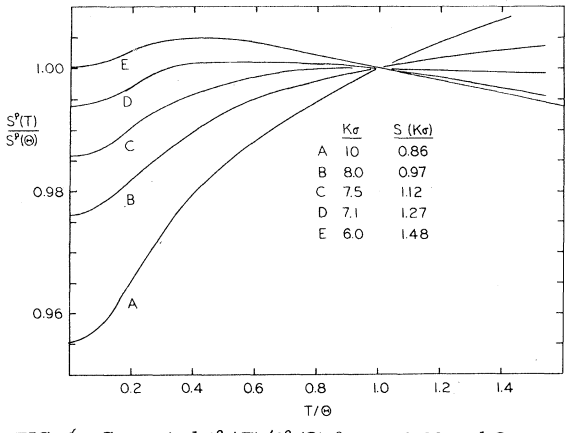

FIG. 3. Computed $S^\rho(T)/S^\rho(\Theta)$ for $\eta = 0.30$ and $\Theta = 340$ K. (The height of the main peak in the structure factor in this case is roughly half that for $\eta = 0.525$.)

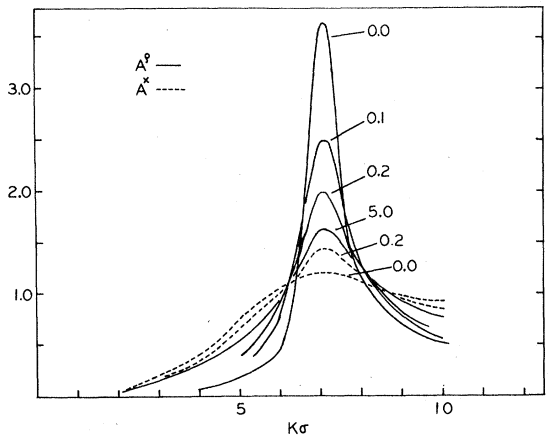

FIG. 4. The averaged structure factors for resistivity $A^\rho(K\sigma)$ and for x-ray scattering $A^x(K\sigma)$ for $\eta = 0.525$ and $\Theta = 340$ K. The reduced temperature T/Θ is indicated for each curve. For $T/\Theta = 5.0$, $A^x(K\sigma)$ is essentially identical to $A^\rho(K\sigma)$. The curves for $T/\Theta = 1.0$, which are not shown, differ from the limiting curve ($T/\Theta = 5.0$) by less than 2%.

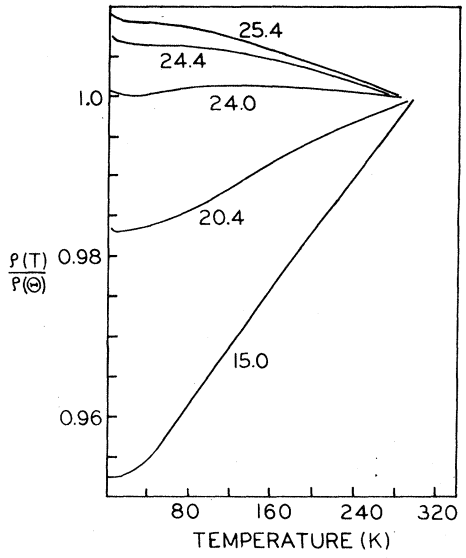

FIG. 5. The resistivity ratio $\rho(T)/\rho(293)$ for amorphous NiP. The phosphorus composition in at.% is indicated on each curve.

$T > \Theta$ is seen to be a crude approximation. It can also be seen that $A^\rho(K) \to A^x(K)$ for $T > \Theta$.

IV. COMPARISON WITH EXPERIMENT

(a) Amorphous NiP: The resistivity data[1] in NiP are shown in Fig. 5. All the measured features are consistent with the predictions of theory as displayed in Fig. 1: (i) the curves exhibit the characteristic S shape; (ii) the largest maximum occurs at $T/\Theta \approx 0.4$ and for the curve at the cross over from positive to negative TCR. The magnitude of this maximum is about 0.2% which compares well with the theoretical value. [Kondo effect makes $\rho(0)$ difficult to determine.]; (iii) the magnitudes of the maxima decrease as the TCR's become more negative and the resistivity becomes larger in accord with theory; and (iv) the magnitudes of the TCR's (positive and negative) at $T \approx \Theta$ are consistent with theory.

These results (Fig. 1) and the experimental results (Fig. 5) determine the range of $2k_F$ in the amorphous NiP alloys. It is thus concluded that $2k_F$ varies from about 2.8 Å^{-1} to about 3.0 Å^{-1} as the phosphorus concentration varies from 15% to 26%. This range of values for $2k_F$ agrees with that employed by Meisel and Cote[5] in an earlier study of the NiP system, which showed that the diffraction model yields (for $T \approx \Theta$) the observed TCR, the magnitude and composition dependence of ρ, and the correct magnitude and sign of the thermopower. Thus, the entire composition and temperature variation of ρ and TCR as well as the magnitude and sign of the room-temperature thermopower are obtained by a consistent application of the diffraction model to NiP. Moreover, the measured temperature dependence of the x-ray structure factor for NiP at $T \gtrsim \Theta$ can be explained in the context of the same structual model.[8]

The related alloy system, amorphous PdCuP,[16] also exhibits a resistivity maximum at the composition near crossover from positive to negative TCR. At higher resistivities, the maxima actually disappear in NiP and PdCuP. This feature has been attributed[17] to the Kondo effect or possible saturation effects which can mask or remove the small maxima (see Sec. V).

(b) Amorphous CuSn: The most thorough study[18] of a system exhibiting the crossover from positive to negative TCR was performed on amorphous vapor-deposited CuSn. CuSn alloys thus provide the best test of the diffraction model. The theoretical results shown in Fig. 1 are in excellent agreement with these data including such details as: (i) the magnitude (percent increase from ρ at $T = 0\ ^\circ K$) and position of the resistivity maxima and their variations with resistivity at Θ, and (ii) the variation of TCR at Θ with ρ at Θ.

The magnitude of the resistivity depends on the appropriate t-matrix elements as well as on structural considerations and is not computed here. However, calculations[12] for liquid CuSn alloys are in good accord with experimental data.[19] Thus, agreement with the experimental data in amorphous CuSn alloys is expected, since structural parameters of liquid and amorphous alloys

are similar.[20] In particular, the data are consistent with a maximum resistivity in both the liquid and amorphous alloys at approximately 70% Cu. The composition dependence of the resistivity is similar although stronger in the amorphous case, as expected, because of the generally sharper features of the structure factors of amorphous solids. Negative TCR's are also common to amorphous and liquid CuSn alloys.

An especially satisfying aspect of application of these ideas to the CuSn alloys pertains to the composition range for which negative TCR's are observed in the amorphous case. From Fig. 1, the range of Fermi wave numbers for which negative TCR's are predicted is given by $\Delta(2k_F)/2k_F \cong 0.20$. Assuming one electron per Cu atom and four electrons per Sn atom, and using the free electron connection between k_F and the electrons per atom ratio $\mathfrak{z}$, the experimental data give $\Delta(2k_F)/2k_F = \Delta\mathfrak{z}/3\mathfrak{z} \gtrsim 0.18$ in excellent agreement with the theoretical prediction.

As a final point consider the thermopower data[18] for amorphous CuSn alloys. The above analysis leads to the conclusion that $2k_F$ ranges from slightly less than K_p, the position of the first peak in the structure factor, for the 80% Cu alloy, to well beyond K_p at the highest Sn compositions. Thus, the diffraction model correctly predicts a transition from positive to negative thermopower as observed upon increasing the Sn concentration in glassy CuSn. The negative thermopower samples do not appear to exhibit the expected linear temperature dependence, however. A sign change is also observed in the thermopower of liquid CuSn alloys.

(c) Amorphous CuZr alloys: Amorphous CuZr alloys have Debye temperatures near 200 K,[21] while the previously discussed systems have $\Theta \approx 300$ K.[22,23] As seen by comparing Fig. 2 with Fig. 1, this leads to larger thermal effects in the resistivity. Anomalous resistivity maxima in CuZrFe alloys were investigated by Szofran *et al.*[9] It was found that these maxima could not be correlated in any straightforward way with anomalies in the magnetic susceptibility. By contrast, the observed shape of the resistivity curves are in excellent agreement with curve *C* of Fig. 2 including the proper magnitude of the peak height [0.25% of $\rho(T=0)$ compared with 0.3% observed], its position at $\sim 0.2\Theta$, and the magnitude of the reduction in ρ from the maxima to Θ. It is also significant that the maxima occur in samples having the smallest high-temperature TCR's. These results indicate that addition of Fe to amorphous CuZr reduces $2k_F$ via electron transfer to Fe *d* states. It is also possible that ferromagnetism in these samples reduces the Kondo effect and its consequent masking of the predicted maxima.

(d) Amorphous noble-metal–polyvalent-metal alloys: Liquid noble-metal–polyvalent-metal alloys[24] yield negative TCR's for

$$\mathfrak{z} = \sum C_i Z_i \simeq 1.5 \text{ to } 2.0 \quad \text{(liquids, empirical)}, \tag{15}$$

where C_i and Z_i are the concentration and effective valence of the ith constituent, respectively.

Korn *et al.*[25] studied vapor deposited amorphous noble-metal–polyvalent-metal alloys and found negative TCR's for a considerably larger range of $\mathfrak{z}$. Thus, it was concluded that the diffraction model could not account for the observed TCR's.

However, our results as embodied in Fig. 1 (and the free electron connection between $\mathfrak{z}$ and $2k_F$) yield, in contrast to the phenomenological result for liquids,

$$\mathfrak{z} = \sum C_i Z_i \simeq 1.3 \text{ to } 3.0 \tag{16}$$

for negative TCR. The role of the averaged structure factor $A^{\rho}(K)$ in determining this negative TCR range is illustrated in Fig. 4. In the light of Eq. (16), it is seen that the data of Korn *et al.*[25] generally support the diffraction model. (Only $Bi_{85}Ag_{15}$ and $Sn_{80}Au_{20}$ yield anomalous TCR's.)

Equation (16) is expected to fail in liquids because of their large thermal expansion and temperature-dependent packing fractions.

V. DISCUSSION

(a) Validity of the diffraction model: The essential validity of the diffraction model for liquid metals has been established.[24] However, large thermal expansion effects and actual atomic rearrangements preclude a simple test of the predictions of temperature-dependent transport effects in liquids.[24] Furthermore, the observed dependence of ρ on T in liquid-transition metals are also explained by competing theories.[26]

The relatively simple temperature dependence of the structure factor of amorphous metals as described in Ref. 8, and the predicted nonlinear effects at $T < \Theta$ make possible a more stringent test of the diffraction model than liquid metals can provide. The theory does remarkably well, giving the temperature dependence of the resistivity of a variety of amorphous metals on a scale of tenths of a percent over the entire accessible temperature range. Such subtle effects as small maxima in the higher resistivity samples, the transition from positive to negative temperature

coefficients of resistivity, and the quadratic temperature dependence of the resistivity at low temperatures are correctly given.

The value of the resistivity is determined by the t-matrix elements as well as the structure factors. However, the t-matrix elements are very sensitive functions of parameters (e.g., E_F) which are difficult to determine a priori. Thus, we examine temperature dependences in this work and do not calculate resistivity magnitudes. It has been demonstrated that reasonable choices of the relevant parameters yield quantitative agreement with the resistivity data in the following examples: (i) the Evans, Greenwood, and Lloyd approximation to $t(K)$ in terms of resonant scattering from d states in liquid transition metals was shown[3] to explain their order of magnitude higher resistivity than that found in simple metals; (ii) Friedel[27] used a similar approach to account for the large resistivities of transition metal impurities; and (iii) Reference 5 reported quantitative agreement with experiment for the resistivity of amorphous NiP alloys.

The original attempt of Cote *et al.*[22] to obtain low-temperature limiting forms for the resistivity of amorphous metals in terms of the diffraction model led to the suggestion of a negative T^2 dependence in some cases. A similar prediction based on a Debye-Waller factor effect was later made by Nagel.[28] These approaches use the x-ray structure factor $S^x(K)$ in place of $S^\rho(K)$ which is not valid for $T<\Theta$. A proper treatment is given in Ref. 6 which gives in all cases the $+T^2$ low-temperature limiting form and the $\pm T$ high-temperature limiting form for ρ. The Debye-Waller factor and the rapidly decreasing value of $A^\rho(K)$ in Eq. (12) produce the observed negative temperature coefficients of resistivity.

Normal scattering, which arises from the $K=0$ singularity[29] in $a(K)$ as in the crystalline case, does not influence the resistivity structure factors $S^\rho(K)$ for $K>q_D$ and is not treated here. We estimate that normal processes contribute less than 1 $\mu\Omega$ cm at Θ and will add a small positive term to the temperature coefficient of resistivity for $T<\Theta$. The general features of the curves in Figs. 1 and 2 will be unchanged.

Frobose and Jackle[29] computed the resistivity of glassy CuSn alloys within the Ziman model. They approximated the structure factors by step functions and used a model pseudopotential. In contrast to our results, they concluded that the observed negative temperature coefficients of resistivity could not be explained by the diffraction model for a Debye-phonon spectrum. The origin of the difficulty with their calculation may lie in their use of a pseudopotential which does not properly weight large angle scattering contributions in Cu.[12,30]

(b) Breakdown of the diffraction model; saturation redefined: It is significant that the resistivities of the alloys discussed range beyond 200 $\mu\Omega$ cm. Mott[26] suggested that the short mean free paths of conduction electrons for such resistivities would lead to breakdown of the diffraction model for liquid-transition metals. Similar suggestions[31-33] for high-resistivity crystalline alloys (including the A-15 group) have led to current controversies concerning the interpretation of transport data in such alloys. The present results imply that saturation effects are not yet appreciable for such resistivities in amorphous alloys. The same can be said of disordered (crystalline) alloys. We have shown[6] that most of the observed transport properties, including adherence to the Nordheim rule and a generalized Norbury-Linde rule, result from application of the diffraction model to disordered transition-metal alloys.

Further support for the essential validity of the diffraction model at high resistivities is found in the transport studies in liquid transition-metal alloys.[12] The general agreement between predicted and observed magnitudes and composition dependences of the electrical resistivity cannot be ignored.

Yet, there exists experimental evidence for saturation at resistivities of the order of 100 $\mu\Omega$ cm. Assuming the correctness of this interpretation[31-33] we are faced with an apparent paradox: the diffraction model breaks down but still yields qualitatively correct results in most cases.

We propose the following resolution of this paradox: as resistivities approach 100 $\mu\Omega$ cm (mean free paths approaching lattice spacings) phonons becomes less effective as scatterers; however, elastic scattering (structure scattering) is still given correctly by the diffraction model. We define this particular type of breakdown of the diffraction model as *saturation*. See Mott[26] for the standard definition.

Thus, in the A-15 metals for which phonon scattering is thought to be dominant, one finds evidence of breakdown of the diffraction model, i.e., saturation, for $\rho<100$ $\mu\Omega$ cm while in amorphous, disordered, and liquid metals for which elastic scattering is dominant, the (unmodified) diffraction model is reliable at higher resistivities. In the latter systems, saturation is a subtle effect and may only be evident in the TCR.

A particularly interesting example is provided by NbGe films.[34] Phonon scattering apparently saturates below 100 $\mu\Omega$ cm, yet increased structure scattering, generated by α-particle bom-

bardment, yields resistivities as large as 200 $\mu\Omega$ cm.

In amorphous alloys with resistivities approaching 200 $\mu\Omega$ cm, the maxima predicted by the diffraction model are generally not seen and the low-temperature resistivity is reported to exhibit a $-T^2$ dependence.[35] Similar behavior has been reported[33] in disordered transition-metal alloys; those having $\rho \gtrsim 150$ $\mu\Omega$ cm display negative TCR at all temperatures with a typical magnitude of 10^{-4} K^{-1}. This is just the behavior produced by *saturation* as defined here. Different explanations of the negative TCR's and the negative T^2 dependences were presented by Nagel[28] and by Markowitz.[36] The anomalous TCR of $Bi_{85}Ag_{15}$ alluded to earlier may be due to this form of saturation. These ideas apply to liquids and explain the large negative TCR's seen in high-resistivity liquid alloys.[26] The present definition of saturation therefore provides a consistent description of the diverse behavior of high resistivity alloys, all within the framework of the diffraction model.

(c) Disordered alloys: The similarities in the behavior of the resistivity of amorphous metals and of disordered alloys were explained in an earlier publication as the result of a common feature of both systems, viz., a continuous structure factor $a(K)$. The similarities of the curves seen in Fig. 3 [where the packing fraction was chosen to give $a(K)$ approximating that seen in disordered Cu_3Au[14]] with those of polycrystalline NiCu alloys[37] suggest a disorder contribution to the observed peaks rather than magnetic effects. The possibility of saturation effects, defined earlier, supports this view. It should also be noted that the short-range-order parameters are themselves temperature dependent which can result in a large enhancement of the predicted effects for $T \gtrsim \Theta$.

(d) Determination of k_F: The curves in Figs. 1–3 imply that ρ is extremely sensitive to the value of k_F. The present results indicate that for complex amorphous systems (including cases where d-level filling is occurring) resistivity and structure factor measurements provide a technique for determining k_F assuming that saturation effects are not large.

[1]P. J. Cote, Solid State Commun. 18, 1311 (1976).
[2]H.-J. Guntherodt, H.-U. Kunzi, M. Laird, R. Muller, R. Oberle, and H. Rudin, in *Proceedings of the Third Conference on Liquid Metals, United Kingdom*, 1976, edited by R. Evans and D. A. Greenwood (Institute of Physics and Physical Society, London, 1977); see also, A. K. Sinha, Phys. Rev. B 1, 4541 (1970).
[3]R. Evans, D. A. Greenwood, and P. Lloyd, Phys. Lett. A 35, 57 (1971).
[4]J. M. Ziman, Philos. Mag. 6, 1013 (1961).
[5]L. V. Meisel and P. J. Cote, Phys. Rev. B 15, 2970 (1977).
[6]P. J. Cote and L. V. Meisel, Phys. Rev. Lett. 39, 102 (1977).
[7]L. V. Meisel and P. J. Cote, Phys. Rev. B 16, 2978 (1977).
[8]P. J. Cote, G. P. Capsimalis, and L. V. Meisel, Phys. Rev. B 16, 4651 (1977).
[9]For a brief review, see, F. R. Szofran, G. R. Gruzalski, J. W. Weymouth, D. J. Sellmyer, and B. G. Giessen, Phys. Rev. B 14, 2160 (1976).
[10]L. Van Hove, Phys. Rev. 95, 249 (1954).
[11]I. Hernandez-Calderone, J. S. Helman, and H. Vucetich, Phys. Rev. B 14, 2310 (1976).
[12]O. Dreirach, R. Evans, H.-J. Guntherodt, and H.-U. Kunzi, J. Phys. F 2, 709 (1972).
[13]J. K. Percus and G. J. Yevick, Phys. Rev. 110, 1 (1958); J. K. Percus, Phys. Rev. Lett. 8, 462 (1962).
[14]G. Baym, Phys. Rev. 135, A1691 (1964).
[15]B. E. Warren, *X-Ray Diffraction* (Addison-Wesley, Reading, Mass., 1969).
[16]G. L. Tangonen, Phys. Lett. A 54, 307 (1975).
[17]P. J. Cote and L. V. Meisel, in *Proceedings of the International Conference on the Physics of Transition Metals, Toronto, Canada*, 1977 (Inst. Phys. Conf. Ser. No. 39, London, 1978).
[18]D. Korn, W. Murer, and G. Zibold, Phys. Lett. A 47, 117 (1974); D. Korn and W. Murer, Z. Phys. B 27, 309 (1977).
[19]A. Roll and H. Motz, Z. Metallkd. 48, 435 (1957).
[20]W. E. Lukens and C. N. J. Wagner, J. Appl. Crystallogr. 9, 159 (1976).
[21]T. Mizoguchi, S. von Molnar, G. S. Cargill III, T. Kudo, N. Shiotani, and H. Sekizawa, in *Amorphous Magnetism II*, International Symposium on Amorphous Magnetism, 2d, Rensselaer Polytechnic Inst., 1976, edited by R. A. Levy and R. Hasegawa (Plenum, London, 1977).
[22]P. J. Cote, G. P. Capsimalis, and G. L. Salinger, in Ref. 21.
[23]Y. S. Tyan and L. E. Toth, J. Electron. Mater. 3, 791 (1974).
[24]T. E. Faber, *Liquid Metals* (Cambridge U.P., London, 1972).
[25]D. Korn, H. Pfeifle, and G. Zibold, Z. Phys. 270, 195 (1974).
[26]N. F. Mott, Philos. Mag. 26, 1249 (1972).
[27]J. Friedel, Can. J. Phys. 34, 1190 (1956).
[28]S. R. Nagel, Phys. Rev. B 16, 1694 (1977).
[29]K. Frobose and J. Jackle, J. Phys. F 7, 2331 (1977).
[30]T. E. Faber, in *Physics of Metals I Electrons*, edited by J. M. Ziman (Cambridge U.P., London, 1969).
[31]Z. Fisk and G. W. Webb, Phys. Rev. Lett. 36, 1084 (1976).
[32]H. Weismann, M. Gurvitch, H. Lutz, A. Ghosh,

B. Schwarz, and M. Strongin, Phys. Rev. Lett. 38, 782 (1977).
[33]J. H. Mooij, Phys. Status Solidi A 17, 521 (1973).
[34]L. R. Testardi, J. M. Poate, and H. J. Levinstein, Phys. Rev. B 15, 2570 (1977).
[35]R. Hasegawa, Phys. Lett. A 38, 5 (1972).
[36]D. Markowitz, Phys. Rev. B 15, 3617 (1977).
[37]R. W. Houghton, M. P. Sarachik, and J. S. Kouvel, Phys. Rev. Lett. 25, 238 (1970).